

Final Technical Report

USGS/NEHRP Award No: 05HQGR0175

Evaluation of Double-difference Algorithms at the NEIC

Principal Investigator: Felix Waldhauser
Co-PI: David Schaff

Lamont-Doherty Earth Observatory of Columbia University
Palisades, NY 10964
Tel: (845) 365 8538; Fax: (845) 365 8150
felixw@ldeo.columbia.edu

Project Period: 01/01/2006 – 12/31/2006

Research supported by the U.S. Geological Survey (USGS), Department of the Interior, under USGS award number 05HQGR0175. The views and conclusions contained in this document are those of the authors and should not be interpreted as necessarily representing the official policies, either expressed or implied, of the U.S. Government.

ABSTRACT

We tested and evaluated a double-difference algorithm for its potential implementation at the NEIC to relocate earthquakes recorded at global seismic network, using differential times formed from first and later arriving phases listed in global seismic bulletins. In addition, we show some initial results from our ongoing project (07HQGR0044) on evaluating time-domain cross correlation methods to improve differential times based on phase picks. In this report we outline some of the methodological developments, and then focus on the performance of the spherical, multi-phase double-difference algorithm using 75 crustal earthquakes in the 1999 Izmit and Düzce, Turkey, aftershock sequences. We find a low level of waveform similarity in this aftershock sequence, and consequently few correlated events, which we attribute to the complexity of both the fault structures and faulting processes. Nevertheless, double-difference solutions based on a combination of differential times from cross-correlation and EHB phase picks are able to image orientation and dip of individual fault segments that are consistent with focal mechanisms and near surface information. Differences between the double-difference locations and corresponding locations in global seismicity catalogs (EDR, ISC, EHB) are typically greater than 10 km. Residual statistics and comparison with accurately known locations indicate mean relative location errors at the 90% confidence level of 2.4 km laterally and 1.8 km vertically. These results indicate that cross-correlation and double-difference methods may be useful to obtain high-resolution event locations within the framework of routine earthquake catalog production at the NEIC.

1. Overview

This report covers the activities performed between January 1, 2006 (start date of the project) and December 31, 2006 on evaluating a global double-difference algorithm to relocate earthquakes using regional and teleseismic phase picks. Note that this project continues in the current year under a different grant number (07HQGR0044), and we have also included some of our latest work in this report on improving pick based differential times using cross correlation methods. The work described here is being undertaken by the principle investigator Felix Waldhauser and by co-PI David Schaff.

2. Investigations undertaken

1) Regional/teleseismic double-difference code to reduce model errors:

Under the FY2006 grant we have adapted, tested, and applied a new double-difference algorithm to relocate earthquakes recorded at regional and teleseismic distances for potential use at the NEIC, using first and later arriving phase travel times. The software is an extensively reworked version of the original algorithm *hypoDD* (Waldhauser, 2001), which relates the residuals between the observed and predicted phase travel time differences for pairs of earthquakes observed at common stations to changes in the vector connecting their hypocenters through the partial derivatives of the travel times for each event with respect to the unknowns (Waldhauser and Ellsworth, 2000). This approach is especially useful in regions with a dense distribution of seismicity, i.e. where distances between neighboring events are small relative to the length scale of the variation in velocity structure. By linking hundreds or thousands of earthquakes together through a chain of nearby neighbors it is possible to obtain high-resolution hypocenter locations over large distances without the use of station corrections.

While the fundamental equations for the teleseismic algorithm are the same as described in Waldhauser and Ellsworth (2000), the new *hypoDD* algorithm includes several options for predicting partial derivatives and travel times, including 3D raytracing in local (cartesian) and regional (spherical) models, the use of standard Earth models (IASP91 or ak135), and the use of station specific models. *hypoDD* now technically allows the simultaneous use of any of these models, providing the flexibility needed to relocate earthquakes at various spatial scales, in areas with various levels of structural information. 3D effects in 1D double-difference solutions have been investigated and quantified in order to validate the use of laterally constant velocity models (Waldhauser and Schaff, submitted to JGR). The original dynamic weighting scheme employed in *hypoDD*, which optimally weights the different data types and qualities during the inversions (Waldhauser, 2001), has been refined and extended to account for additional factors typical to global phase data such as the ambiguity in phase identification near cross-over distances.

2) Waveform Cross Correlation to Improve NEIC Phase Picks

Under the current grant (FY2007) that started in January 2007 we are developing a cross-correlation algorithm to compute accurate differential arrival times for globally observed phases of pairs of closeby events recorded at common stations. Cross-correlation methods take advantage of the fact that two earthquakes that are close in space and have similar focal mechanisms produce similar seismograms at common stations (Poupinet et al., 1984). Cross-correlation methods can then measure differential phase arrival times with sub-sample precision, typically resulting in more than an order of magnitude improvement over phase onset picks in

earthquake bulletins (e.g., Poupinet et al., 1984; Schaff et al., 2004). Since the double-difference method uses differential times directly, events with correlated seismograms are relocated to the accuracy of the cross-correlation data while events that do not correlate are determined to the accuracy of the phase pick data.

We have successfully applied our time domain cross correlation algorithm (Schaff et al., 2004) to first arriving P- and S-waves recorded at local distances (e.g., Schaff and Waldhauser, 2005), regional phases (Schaff and Richards, 2005), and teleseismic phases of selected earthquakes (Zhang et al., 2005; Zhang et al., 2007) and nuclear explosions (Waldhauser et al., 2004). We are in the process of reworking these tools so they can be applied to large numbers of earthquakes and stations, using waveforms obtained from IRIS and recorded at stations around the world. We have implemented STA/LTA filters that precede the correlations in order to reduce the number of noise-correlations and improve the robustness of the differential time measurements. This has proven especially useful when using theoretical predictions to find the arrival times of the phases we like to correlate in cases where there are not picks in the bulletin.

The performance of these tools is best shown using an example of 359 events that occurred in the subducting Nazca plate beneath Northern Chile. We performed 56,621 ‘black-box’ cross correlations at 998 stations, from which 7318 P- and 567 S-waves have a cross correlation coefficient (CC) > 0.7. The cross correlations were performed on a 10 s window surrounding the first arriving P- or S-waves. Lags searched over are plus and minus 5 s. Examples of cross-correlated seismograms are shown in Figure 1 for phases observed at regional (station ZOBO, Bolivia) and teleseismic (ANMO, USA; WMQ, China) distances. Superimposed on the aligned waveforms are the EHB bulletin phase picks that demonstrate the two main benefits of using waveform cross correlation: the reduction in the scatter in phase onset picks (ZOBO, WMQ), and the measurement of additional delay times of phases not picked by analysts. The standard deviation of the scatter in the analyst picks is 1.7 s at station ZOBO, 0.14 s at station WMQ, and 0.03 s at station ANMO (note that station ANMO has only two picks). Errors in the correlation measurements based on an evaluation of the internal consistency is on the order of 0.01 s or less. For WMQ this represents about one order and for ZOBO two orders of magnitude improvement over differential times formed from phase picks. The improvement in differential time accuracy translated to relative location errors of 2 km horizontally and 1.4 vertically for correlated events, compared to an average of 3.5 km and 2.1 km when all double-difference locations are considered (Waldhauser and Schaff, *subm. to JGR*). Median horizontal and vertical location differences between our cross-correlation based double-difference locations and the ISC locations are 15 and 132 km, respectively. Differences to the EHB locations are 12 km in both directions, within the range of the estimated average EHB location uncertainty (10-15 km, Engdahl et al., 1998).

Both the cross-correlation and double-difference tools have been developed for application in ‘black-box’ operation on large amount of data. This required the developemnt of efficient outlier detection routines that operate before and during the double-difference inversions. We describe both method improvements and application to subduction and crustal earthquake in a paper that we submitted to JGR in January 2007. In the following we present the application most crucial to the NEIC, i.e. crustal earthquakes in the 1999 Izmit/Duezce aftershock sequence, and demonstrate performance and location precision using ‘ground truth’ events, focal mechanisms, and near surface information.

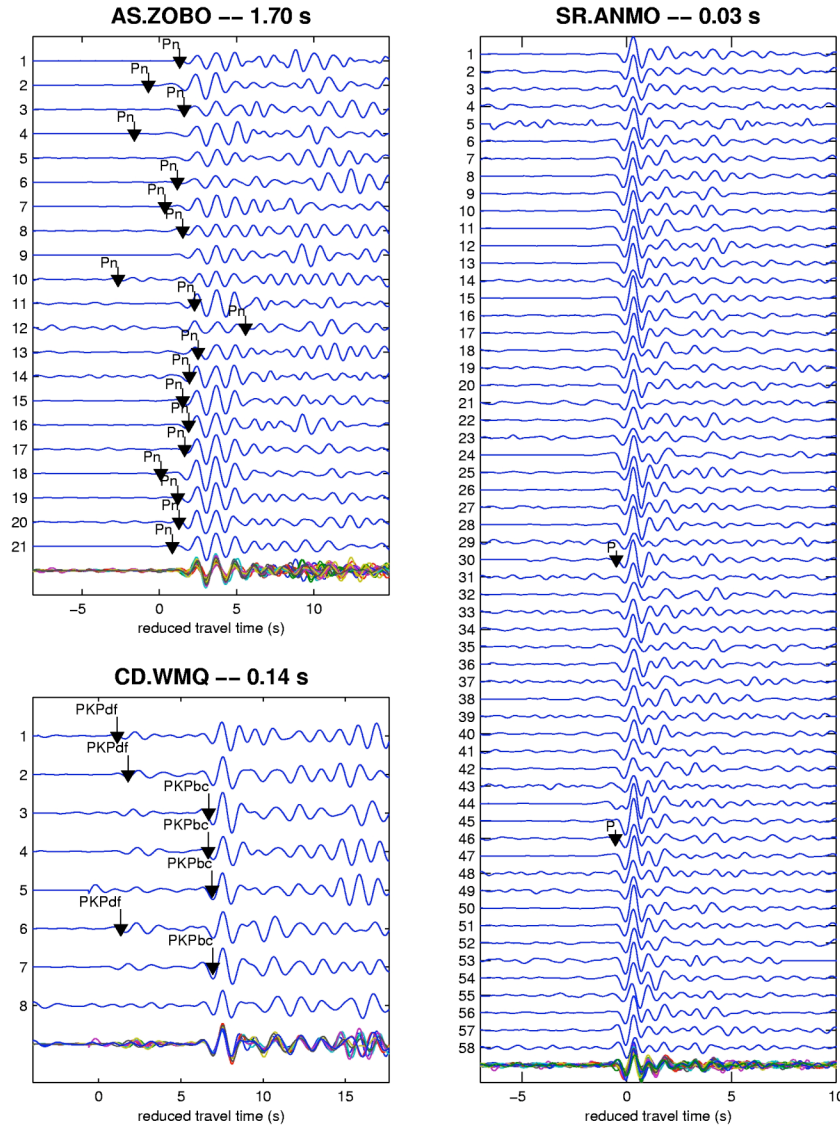
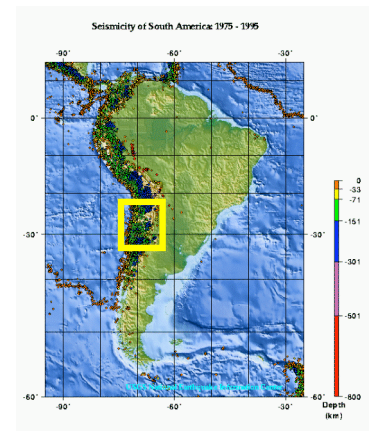


Figure 1 Filtered (0.1-2 Hz) and cross-correlation aligned waveforms of selected events in the Nazca plate beneath Northern Chile (see below) recorded at regional (ZOBO) and teleseismic (ANMO, WMQ) stations. Phases observed at ANMO are bottoming in the lower mantle, those at WMQ in the core. Bottom line in each panel superimposes traces shown above, arrows indicate arrival-time picks available from the EHB bulletin.



2. Results

Evaluation using the Izmit and Duzce earthquake sequence of 1999

We choose 75 events in the 1999 Izmit-Düzce earthquake sequence to investigate the performance of the global cross-correlation based double-difference algorithm to relocate hypocenters in the Earth's crust. The events span a distance of nearly 200 km along the northernmost strand of the North Anatolian fault system, making them well suited to investigate the effect of fault structure, interevent distances, and waveform similarity on double-difference solutions. The Izmit Mw 7.4 mainshock occurred on 17 August 1999 and was centered at 40.748 N., 29.864 E at a depth of 17 km (USGS). It ruptured approximately 60 km of the surface in an

almost pure right lateral strike slip fashion (USGS CMT: strk=95, dip=81, slip=180; Harvard CMT: strk=91, dip=87, slip=164). On 12 November 1999 a second earthquake with Mw 7.1 occurred about 100 km to the east of the Izmit event near the village of Düzce, at 40.758 N 31.161 E and 10 km depth (USGS). Again, CMT solutions indicate almost pure right lateral strike slip (USGS CMT: strk=269, dip=73, slip=177; Harvard CMT: strk=268, dip=54, slip=167). These two mainshocks and 40 aftershocks ($3.8 < M_w < 5.8$) from the Izmit event and 33 aftershocks ($4.0 < M_w < 5.5$) from the Düzce event are used in our relocation analysis.

We use phase picks and initial locations as listed in the EHB bulletin (Engdahl et al., 1998; Bob Engdahl, pers. comm.). From a total of 11,780 first and later arriving P and S body wave phase picks, 91,783 picks have been pair wise observed at common stations (Figure 2). Ten stations are within local distances (<200 km) from the cluster centroid, most of them locating south of the fault and therefore causing a primary station gap $>180^\circ$ for most of the 75 events. 71 events were recorded at one or more local stations, 37 events at 4 or more local stations. 227 stations are within regional distances (<2000 km), with most stations located in Greece and western Europe. 383 stations recorded the events at teleseismic distances (>2000 km). We have sub-sampled the station distribution for each event pair in order to avoid strong spatial clustering of partial derivatives in areas with dense seismic networks (e.g., arrays or local networks reporting to the ISC). We select only the best station (i.e., the highest quality pick) within bins of $3^\circ \times 3^\circ$ beyond a distance of 200 km from the cluster centroid.

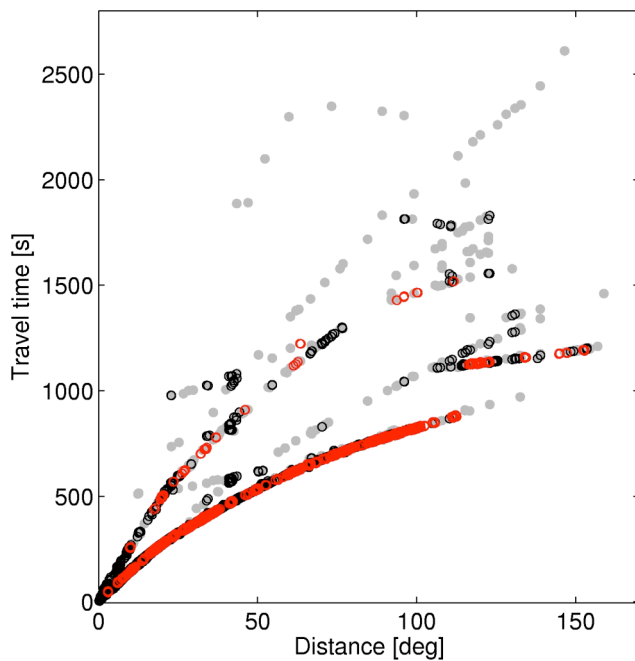


Figure 2 Phase travel times as a function of distance for the 75 earthquakes in the Izmit-Düzce sequence. Gray dots denote original EHB bulletin picks, black circles pairwise observed picks, and red circles phases for which cross correlation measurements were obtained.

In addition to the phase pick data we compute accurate differential times by performing a total of 21,812 cross correlations on 561 filtered (0.1-2 Hz) seismograms obtained from the IRIS DMC, using the time-domain method of Schaff et al. (2004). We choose window lengths of 10 s around the predicted P, PKP, S, and SKS phase arrival time, and searched over lags of 5 s. Similar to the Chile application a STA/LTA filter (1s/5s) is applied to the seismograms before the correlation measurements were carried out. A total of 1,977 P-wave and 49 S-wave correlations had correlation coefficients $CC > 0.7$. The percentage of similar event pairs is 9% which is less than that for the Chile earthquakes (14%). Most of the events that correlate can be grouped into doublets and triplets. Careful inspection of seismograms for pairs of events that are closely indicate that, even though their hypocenters are close together, the waveforms observed at common stations are dissimilar, suggesting that variation in source mechanisms may be the reason for the low percentage of correlation measurements (see below).

Relocation and residual analysis

A series of 50 dynamically weighted damped least-square iterations is used to simultaneously relocate the 75 events using the combined pick and correlation data. Interevent distance thresholds are gradually decreased from 180 km during the first to 25 km during the final iterations. We invert for all hypocentral parameters (including depths) except for the depths of the two mainshocks, which we fix at 17 km for the Izmit and 10 km for the Düzce shock. Note that most depths in the EHB catalog are fixed at a default value of 10 km. Before relocation, the number of links established between each event and its neighboring events in the cluster range from 759 to 4046. During relocation the data is reduced by the weighting function to between 73 and 1326 highest quality links per event. The double-difference results are shown in Figure 3 in a map view and three cross sections. Ellipses in Figure 3a and crosses in Figure 3b indicate 90% confidence levels obtained from a bootstrap analysis of the final double-difference vector. Error ellipses are mostly elongated in north-north-east direction, consistent with a lack of local and regional stations north of the fault. Mean location uncertainties are 3 km laterally and 4 km vertically. Mean horizontal and vertical shifts between the initial (EHB) and relocated locations are 4.5 km and 5.1 km, respectively.

The data set presented here is well suited to investigate some of the key features of the double-difference method. While JHD (Douglas, 1967; Frohlich, 1979) or HDC (Jordan and Sverdrup, 1981) methods reference partial derivatives relative to the cluster centroid, their applications are limited to earthquake clusters that have spatial dimension that are typically smaller than the length scale of the velocity heterogeneity encountered by all rays between the source region and a common station (typically several km). The double-difference method, on the other hand, references partial derivatives at each hypocenter with respect to a particular station, thus using differential times directly to solve for event separations. This approach allows large areas of seismicity to be relocated simultaneously, as long as there exists a continuous link between events over distances smaller than the length scale of structural heterogeneities encountered by the two rays of linked events traveling to a common station. Larger residuals and bias in double-difference solutions are therefore expected for events linked over large distances.

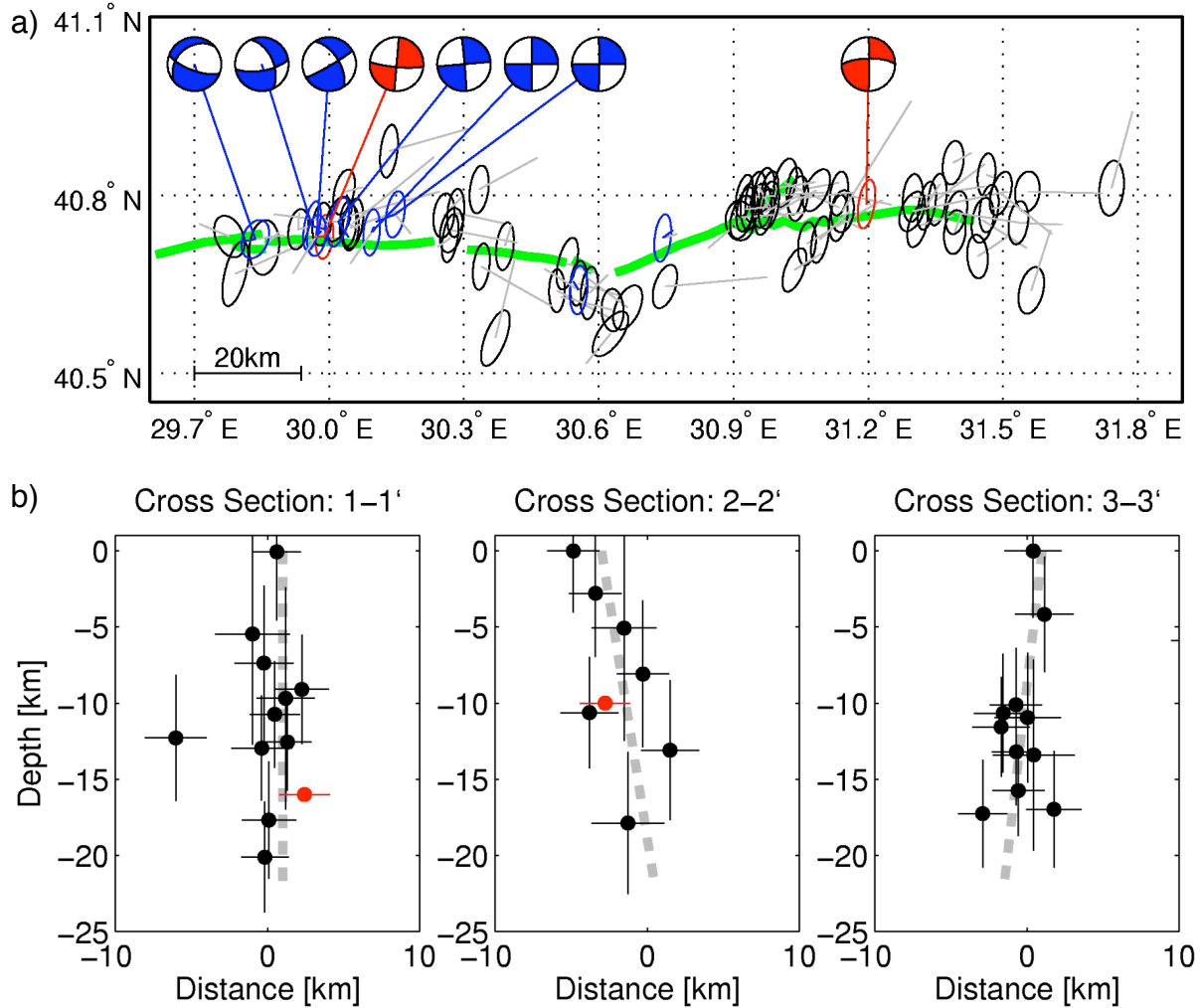


Figure 3 Double-difference locations in a) map view and b) fault perpendicular cross sections for the 75 events in the Izmit-Düzce sequence. Error estimates at the 90% confidence level are represented by ellipses in (a) and crosses in (b). The Izmit and Düzce mainshocks are shown in red, the GT2 events of Özalaybey et al. (2002) in blue. Gray lines connect DD locations to corresponding initial locations taken from the EHB catalog, red and blue lines to mainshock and GT2 locations, respectively. Focal mechanisms are shown for the two mainshocks (red) (USGS CMT) and for 6 GT2 events (blue) (Özalaybey et al., 2002). Boxes in a) indicate location and orientation of cross sections shown in b). Green line in a) denotes surface trace of the fault rupture (from Pucci et al., 2006). Dashed gray lines in b) represent fault dip inferred from relocated aftershocks.

The increase in differential time residuals with increasing interevent distances is shown in Figure 4. RMS residuals are computed for each event and its linked neighboring events for a series of double-difference runs with maximum interevent distance thresholds between 20 km and 180 km, and then plotted as a function of distance along the fault. A constant increase in the average RMS residual from about 0.7 sec (20 km) to 1 sec (180 km) is observed, as increasingly different

ray paths introduce model errors that originate from outside the source region. Note that these results are obtained with the distance weighting function still activated, thus data that link together events over larger distances are downweighted. If no distance weighting is used, and data links of up to 180 km are allowed, then the average RMS residual jumps to 1.3 sec (Figure 4). A small trend towards higher residuals for the Düzce aftershocks compared to the Izmit aftershocks may indicate the higher complexity of fault structures along this segment of the North Anatolian fault.

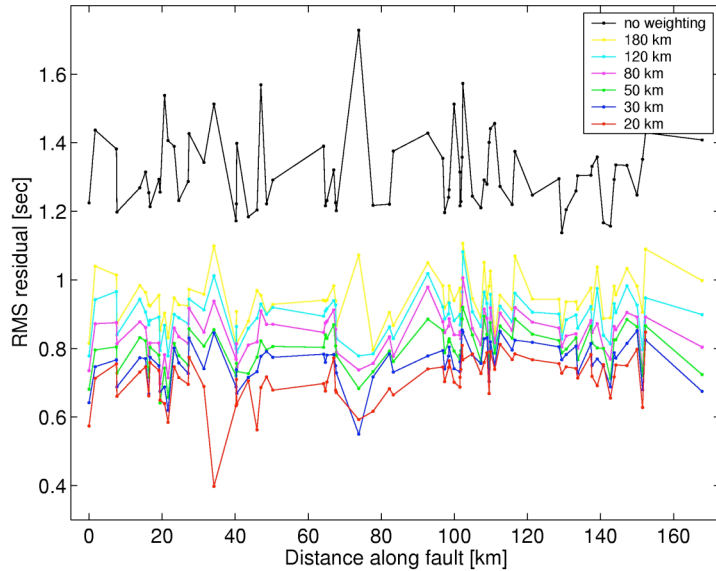


Figure 4 RMS of differential time residuals shown for each event as a function of distance along the fault. Residual curves are shown for a series of double-difference inversions with different interevent distance cutoff values.

Evaluation using ground truth data

We evaluate the accuracy of the relocation results with respect to locations of events determined in special studies using dense local networks (Özalaybey et al., 2002) and with respect to near-surface geologic information (Pucci et al., 2006). A detailed study of the Izmit aftershock sequence by Özalaybey et al. (2002) produced an aftershock catalog (RMS = 0.16 s) with average horizontal and vertical errors of 1.7 km and 2.3 km, respectively, rendering them ground truth at the 2 km level (GT2). From a list of 27 well-located larger magnitude aftershocks (Özalaybey et al., 2002, their Table 2), 6 events, located near the mainshock between 29.8 E and 30.2 E., are also among the 75 events studied here. Accurate locations of an additional two events determined from recordings at a local temporary seismic network (N. Seeber and J. Armbruster, pers. communication) are also used for comparison. The first event is an aftershock of the Izmit mainshock and locates at approximately 30.55 E in Figure 3a slightly south of the surface trace. The second is an aftershock of the Düzce mainshock and occurred at 30.75 E close to the fault. Comparing these accurate local network locations with their corresponding double-difference solutions results in mean horizontal and vertical differences of 2.4 km and 1.9 km, respectively. Except for one event, all corresponding 90% coverage ellipses overlap.

A comparison between the double-difference solutions and locations listed in the catalogs of the EDR, ISC, and the EHB are shown in Figure 5a and b. Median (mean) horizontal/vertical differences are 7.2/4.5 (8.6/5.3) km for EDR, 4.8/5.4 (6.4/6.1) km for ISC, and 8.2/4.5 (8.1/5.6)

km for EHB locations. Note that most events in the EHB and EDR catalogs have depths fixed at default values. Figure 5c and d show the horizontal and vertical distribution of mislocations for the 9 events relative to the local network solutions of Özalaybey et al. (2002). The median (mean) horizontal mislocation are 3.9 (5.5) km for the EDR, 3.3 (3.3) km for the ISC, and 6.4 (6.8) km for the EHB locations. These values are significantly greater than the median (mean) horizontal mislocation of 2.6 (2.4) km for the double-difference solutions.

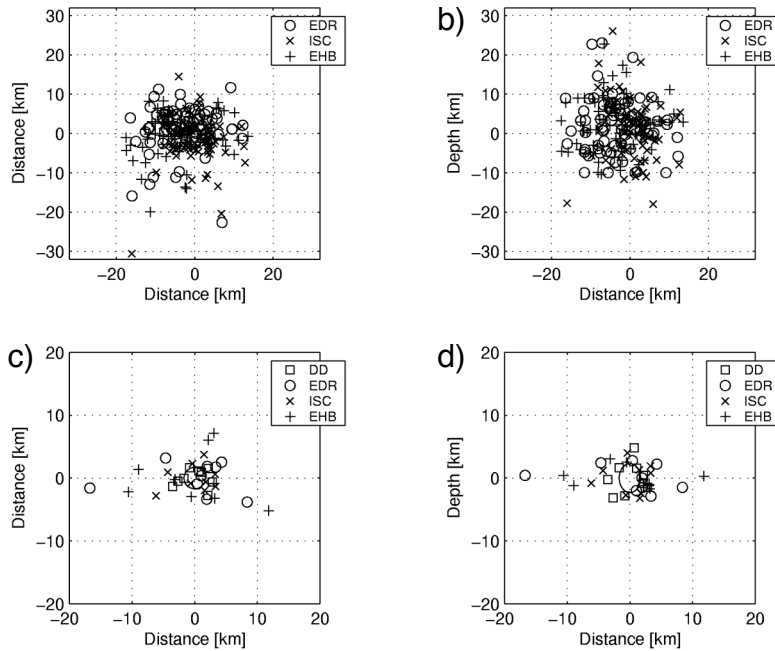


Figure 5 Horizontal (a) and vertical (b) distribution of differences between the 75 DD locations and their corresponding locations listed in the EDR, ISC, and EHB catalogs. Horizontal (c) and vertical (d) differences between the 9 GT2 locations of Özalaybey et al. (2002) and the DD, EDR, EHB, and ISC locations. Ellipses indicate the approximate average error of the GT2 events.

Evaluation using information on fault structures

The overall pattern of the relocated aftershocks of both the Izmit and Düzce mainshocks correlate with the general trend of the surface trace (Figure 3a). The scatter in the epicenter distribution likely reflects the complex rupture of both events, as evident from surface expressions of the main ruptures (Barka et al., 2002; Akyüz et al., 2002; Pucci et al., 2006) and the variation of focal mechanisms. Relocated aftershocks near the Izmit hypocenter indicate a 20 km deep, near vertical fault (cross section 1-1', Figure 3b) consistent with the focal mechanisms of the mainshock (red, Figure 3a) and those of three aftershocks east of the main shock (blue, Figure 3a; Özalaybey et al., 2002). The width of the seismically imaged fault is not resolvably different from zero. A large variation in focal mechanisms is observed for three aftershocks west of the mainshock.

In a recent study, Pucci et al. (2006), based on detailed geologic mapping, inferred a rather complex structure of the fault associated with the Düzce earthquake sequence. Of particular interest to this study is their finding of a south dipping fault of the Cinarli segment on which the mainshock occurred, and a north dipping fault for the adjacent Yenikoy segment to the west. Their results are consistent with fault perpendicular cross sections of our aftershock locations along these segments. Aftershocks along the Cinarli segment (Figure 3b, cross section 2-2') indicate a 10° south dipping fault, while aftershocks along the Yenikoy segment an

approximately 5° north dipping fault (cross section 3-3'). The situation along the Yenikoy segment is complicated as some of the events may have reactivated a strand that ruptured during the Izmit event slightly to the north of the Yenikoy segment.

The general complexity of the fault structure, expressed by the aftershock locations, the variation in focal mechanisms and the complex surface ruptures, appears to be the main reason for the low number of earthquakes with similar waveforms at common stations, and thus the relatively low number of cross-correlation differential time measurements. However, the combination of phase pick and available cross-correlation data is sufficient to resolve relative depths to the extent that we can image strike and dip of active fault planes from aftershock data recorded at global seismic networks.

4. References

- Akyüz, H. S., R. Hartleb, A. Barka, E. Altunel, G. Sunal, B. Meyer, and R. Armijo (2002), Surface Rupture and Slip Distribution of the 12 November 1999 Düzce Earthquake (M 7.1), North Anatolian Fault, Bolu, Turkey, *Bull. Seism. Soc. Am.*, 92, 61-66.
- Barka, A., H. S. Akyüz, E. Altunel, G. Sunal, Z. Çakir, A. Dikbas, B. Yerli, R. Armijo, B. Meyer, J. B. de Chabaliere, T. Rockwell, J. R. Dolan, R. Hartleb, T. Dawson, S. Christofferson, A. Tucker, T. Fumal, R. Langridge, H. Stenner, W. Lettis, J. Bachhuber, and W. Page (2002), The Surface Rupture and Slip Distribution of the 17 August 1999 Izmit Earthquake (M 7.4), North Anatolian Fault, *Bull. Seism. Soc. Am.*, 92, 43-60.
- Dodge, D., G. C. Beroza, and W. L. Ellsworth, Evolution of the 1992 Landers, California, foreshock sequence and its implications for earthquake nucleation, *J. Geophys. Res.* 100, 9865–9880, 1995.
- Douglas, A. (1967), Joint epicenter determination, *Nature*, 215, 47–48.
- Engdahl, E.R., R. van der Hilst, & R. Buland, Global teleseismic earthquake relocation with improved travel times and procedures for depth determination, *Bull. Seism. Soc. Am.*, 22, 2317-2320, 1998.
- Frohlich, C. (1979), An efficient method for joint hypocenter determination for large groups of earthquakes, *Computers and Geosciences* 5, 3–4, 387–389.
- Got, J.-L., J. Frechet, and F. W. Klein, Deep fault plane geometry inferred from multiplet relative relocation beneath the south flank of Kilauea, *J. Geophys. Res.* 99, 15,375–15,386, 1994.
- Jordan, T. H., and K. A. Sverdrup (1981), Teleseismic location techniques and their application to earthquake clusters in the South-Central Pacific, *Bull. Seism. Soc. Am.*, 71, 1105–1130.
- Özalaybey, S., M. Ergin, M. Aktar, C. Tapirdamaz, F. Biçmen, and A. Yörük (2002), The 1999 Izmit Earthquake Sequence in Turkey: Seismological and Tectonic Aspects, *Bull. Seism. Soc. Am.*, 92, 376-386.
- Poupinet, G., W. L. Ellsworth, and J. Frechet, Monitoring velocity variations in the crust using earthquake doublets: An application to the Calaveras Fault, California, *J. Geophys. Res.*, 89, 5719-5713, 1984.
- Pucci, S., N. Palyvos, C. Zabcı, D. Pantosti, and M. Barchi (2006), Coseismic ruptures and tectonic landforms along the Düzce segment of the North Anatolian Fault Zone (Ms 7.1, November 1999), *J. Geophys. Res.*, 111, B06312, doi:10.1029/2004JB003578.
- Rubin, A.M., D. Gillard, and J.-L. Got, Streaks of microearthquakes along creeping faults, *Nature*, 400, 635-641, 1999.
- Rietbrock, A. & F. Waldhauser, A narrowly spaced double-seismic zone in the subducting Nazca plate, *Geophys. Res. Lett.*, 31, L10608, doi:10.1029/2004GL019610, 2004.

- Schaff, D.P., G.H.R. Bokelmann, G.C. Beroza, F. Waldhauser, and W.L. Ellsworth, High resolution image of Calaveras Fault, California, seismicity, *J. Geophys. Res.*, 107, 2186, doi:10.1029/2001JB000633, 2002.
- Schaff, D. P., G.H.R. Bokelmann, W.L. Ellsworth, E. Zankerka, F. Waldhauser, and G. C. Beroza, Optimizing correlation techniques for improved earthquake location, *Bull. Seism. Soc. Am.*, 94, 705-721, 2004.
- Schaff, D. P., and P. G. Richards, Lg-wave cross correlation and double-difference location: application to the 1999 Xiuyan, China, sequence, *Bull. Seism. Soc. Am.*, 94, 867-879, 2005.
- Schaff, D.P. and F. Waldhauser, Waveform Cross-Correlation-Based Differential Travel-Time Measurements at the Northern California Seismic Network, *Bull. Seism. Soc. Am.*, 95, 2446-2461, 2005.
- Waldhauser, F., W.L. Ellsworth, and A. Cole, Slip-Parallel Seismic Lineations on the Northern Hayward Fault, California, *Geophys. Res. Lett.*, 26, 3525-3528, 1999.
- Waldhauser, F., and W.L. Ellsworth, A double-difference earthquake location algorithm: method and application to the northern Hayward Fault, California, *Bull. Seism. Soc. Am.*, 90, 1,353-1,368, 2000.
- Waldhauser, F., HypoDD: A computer program to compute double-difference hypocenter locations, *U.S.G.S. open-file report*, 01-113, Menlo Park, California, 2001.
- Waldhauser, F., W.L. Ellsworth, D.P. Schaff, & A. Cole, Streaks, multiplets, and holes: High-resolution spatio-temporal behavior of Parkfield seismicity, *Geophys. Res. Lett.*, 31, L18608, doi:10.1029/2004GL020649, 2004a.
- Waldhauser, F., D. P. Schaff, P.G. Richards, & W.-Y. Kim, Lop Nor revisited: nuclear explosion locations, 1976-1996, from double-difference analysis of regional and teleseismic data, *Bull. Seism. Soc. Am.*, 94, 1879-1889, 2004b.
- Waldhauser, F. and D.P. Schaff, Regional and teleseismic double-difference earthquake relocation using waveform cross correlation and global bulletin data, submitted to JGR.
- Wolfe, C.J., P.G. Okubo & P.M. Shearer, Mantle fault zone beneath Kilauea volcano, Hawaii, *Science*, 300, 478-480, 2003.
- Zhang, J., X. Song, Y. Li, P.G. Richards, X. Sun, & F. Waldhauser, Inner core differential motion confirmed by earthquake waveform doublets, *Science*, 309, 1357-1360, 2005.
- Zhang, J., F. Waldhauser, P.G. Richards, and D.P. Schaff, Double-difference relocation of an earthquake nest at Bucaramanga, Colombia: Revelation of a vertical fault at intermediate depth, SSA Annual Meeting, Hawaii, *Seism. Res. Lett.*, 78(2), 2007.

5. Papers/abstracts published related to this project

- Waldhauser, F. and D.P. Schaff, Regional and teleseismic double-difference earthquake relocation using waveform cross correlation and global bulletin data, submitted to JGR, January 2007.
- Waldhauser, F., H. Abend, D. Bohnenstiehl, W. Kim, P. Richards, D. Schaff, M. Tolstoy, Fine-scale Seismicity of Earth's Interior: Regional- and Global-scale Double-difference Applications to Study Plate-tectonic Processes, SSA Annual Meeting, San Francisco, *Seism. Res. Lett.*, 77 (2), 2006.
- Zhang, J., F. Waldhauser, P.G. Richards, and D.P. Schaff, Double-difference relocation of an earthquake nest at Bucaramanga, Colombia: Revelation of a vertical fault at intermediate depth, SSA Annual Meeting, Hawaii, *Seism. Res. Lett.*, 78(2), 2007.